- Technical Paper -

FLEXURAL BEHAVIOR OF PRE-TENSIONED PC BEAMS WITH RUPTURED STRANDS STRENGTHENED BY CFRP SHEETS

Thi Thu Dung NGUYEN[*1], Koji MATSUMOTO[*2], Asami IWASAKI[*3] and Junichiro NIWA[*4]

ABSTRACT

The study on effects of externally bonded CFRP sheets on flexural capacities of prestressed concrete beams with ruptured strands has been conducted. The experimental results revealed the effective performances of bonded CFRP sheets in improvement of the flexural capacity of prestressed concrete beams including ruptured strands. Increasing of the sheet lengths and providing U-shaped anchorages have not shown noticeable influences on the flexural capacities but enhanced the beam stiffness and delayed debonding process.

Keywords: externally bonded CFRP sheet, flexural capacity, prestressed concrete, strand rupture

1. INTRODUCTION

Because of high performance with high strength, durability, and small section, prestressed concrete (PC) has been used widely for infrastructures, especially long span bridge girders. Recently, the deterioration of PC beams due to chloride attacks, insufficient grouts and external impacts that leads to the rupture of strands or tendons has become a concern in many countries. These damages required not only an emergency structural inspection but also a practical repair and strengthening. Many conventional methods may be used to address these problems such as internal splices, external post-tensioning tendons or steel jackets [4]. Unfortunately, implements of these methods consume much time, labors and on the other hand, the strengthening materials themselves may not be protected from future corrosion. Thus, a plausible technique needs to be studied.

Since fiber reinforced polymers (FRPs) were invented in Japan in 1980s, the application of various FRP types (bars, sheets, laminates, etc.,) in structural repair and strengthening has been developed increasingly. Carbon fiber reinforced polymer (CFRP) is a type of FRPs, which is a polymer matrix composite material reinforced by carbon fibers. CFRP sheets have the advantages of high strength to weight ratio; excellent corrosion resistance; ease to construction; aesthetic appearance; and less impact to the environment. Many studies have focused on the application of CFRP sheets in strengthening reinforced concrete structures. It is certain that externally bonded CFRP sheets have a potential for enhancement of the flexural capacity of reinforced concrete beams [6, 7]. Additionally, the guidelines or recommendations for design and construction of externally bonded FRP system have been developed and released in America, Japan and other countries. ACI 440.2R [1] has proposed the design equations for flexural strengthening including PC members. Even though, the effects of high concrete strength on behavior of FRP strengthened members, maximum crack width, deflection prediction and control have not been developed.

The purpose of this study is to evaluate the feasibility of using externally bonded CFRP sheets for repair and strengthening of pre-tensioned PC beams with ruptured strands. Total of eight specimens had been tested to evaluate the loss in flexural capacities due to the loss of strand areas, and to investigate flexural behaviors of PC beams strengthened with CFRP sheet. The experimental parameters were the number of ruptured strands, length of CFRP sheet, and presence of U-shaped anchorage for CFRP sheet. Furthermore, this paper compared the experimental results with the predicted values based on ACI codes and guides [1, 2].

2. EXPERIMENTAL PROGRAM

2.1 Test specimens

(1) Specimen details

The eight beams, rectangular-section of 150 mm wide by 300 mm height and 3300 mm long, were cast. The details of specimens are shown in Fig. 1. Four of seven-wire prestressing strands of 10.8 mm diameter, which cross-section area of each strand is 70.08 mm^2, were used. The initial prestressing stress of 1075 N/mm^2 was provided for each strand. The differences of concrete sections at middle of span (section A) are shown in Fig. 1. Deformed bar stirrups of 10 mm nominal diameter were provided to prevent from shear failures. The specimens included a control beam (CB); five beams with one cut strand (DB1) and two beams with two cut strands (DB2). In order to simulate the damage status of beams, a portion of concrete section with the length of 100 mm and height of 50 mm was

*1 Graduate student, Dept. of Civil Engineering, Tokyo Institute of Technology, JCI Member
*2 Assistant Prof., Dept. of Civil Engineering, Tokyo Institute of Technology, Dr. E., JCI Member
*3 Civil Technical Section, Civil Engineering Division, Fuji P.S Corporation
*4 Prof., Dept. of Civil Engineering, Tokyo Institute of Technology, Dr. E., JCI Member

Table 1 Material properties

Concrete	Prestressing strands			Steel
f'_c (N/mm^2)	f_{pu} (N/mm^2)	f_{py} (N/mm^2)	E_{ps} (N/mm^2)	f_y (N/mm^2)
58.4	1,841	1,669	190,000	375

f'_c: compressive strength of concrete; f_{py} and f_{pu}: yielding and ultimate strength of strand; E_{ps}: elastic modulus of strand; f_y: yielding strength of steel;

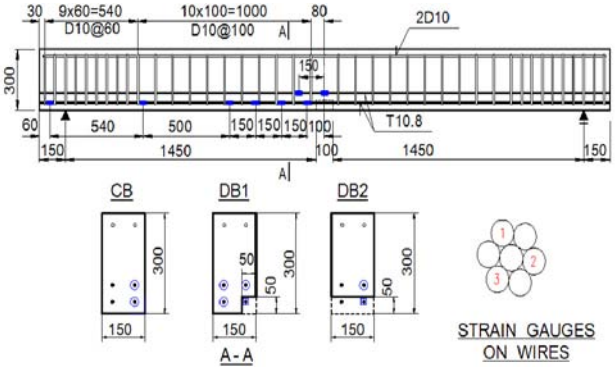

Fig.1 Details of specimens

left at the middle of span in case of DB1 and DB2. After 28 days of casting concrete, the prestressing strands were cut at the middle of span. The concrete sections, then, were restored to the original rectangular ones by cementitious mortar whose 28-day compressive strength is 58.2 N/mm^2. The strain gauges were bonded to the prestressing strands in terms of measuring strains before, after cutting and during the loading test. The solid rectangles denote the locations where strain gauges were attached to prestressing strands [Fig.1]. There were six locations where strain gauges were attached in cut strands and two locations in uncut strands. At each location, three strain gauges were attached on wires, the strain at one location was taken the average values obtained from these three measurements. The designed material properties of specimens are given in Table 1.

(2) Strengthening schemes

Fig. 2 shows the layout of strengthened beams with externally bonded CFRP sheets. The experimental cases are listed in Table 2. Except CB, the other specimens can be divided into two series: (1) the beams with one strand cut including DB1, DB1-100, DB1-200, DB1-284, DB1-100U; and (2) the beams with two cut strands including DB2 and DB2-100. CB, DB1 and DB2 were the reference specimens, which were not strengthened by CFRP sheets. In the other five beams, one layer of CFRP sheets was attached to the bottom of the beams for flexural strengthening. The different length of CFRP sheets (in centimeter unit) is denoted in the name of cases. U-shaped anchorages were provided at both ends of the CFRP sheet in case DB1-100U in order to delay the sheet peeling. CFRP sheets with thickness of 0.111 mm, tensile strength of 3,400 N/mm^2 and Young's modulus of 2.3x10^5 N/mm^2 were used. CFRP sheets were applied by the wet-layup procedure. The specimens were cured in room temperature for at least seven days before the loading test.

Table 2 Experimental cases

Name	Strand loss area	CFRP			
		n_f	b_f (mm)	l_f (mm)	w_f (mm)
CB	-	-	-	-	-
DB1	25%	-	-	-	-
DB2	50%	-	-	-	-
DB1-100	25%	1	125	1,000	-
DB1-200	25%	1	125	2,000	-
DB1-284	25%	1	125	2,840	-
DB1-100U	25%	1	125	1,000	180
DB2-100	50%	1	125	1,000	-

n_f: number of layer; b_f: width of CFRP sheet; l_f: length of CFRP sheet; w_f: width of transverse U-shaped CFRP sheet;

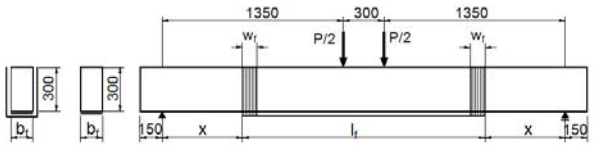

Fig.2 Layout of externally bonded CFRP sheets

2.2 Loading method

The specimens were tested statically in a four-point bending to failure. Mid-span displacements were measured using linear variable differential transducers (LVDTs). The strain gauges were attached to measure the strains at top fiber of concrete at mid span and along CFRP sheets. Crack openings in the constant moment region were measured using Pi gauges. During the loading test, crack propagations were marked with the applied load.

3. RESULTS AND DISCUSSIONS

3.1 Flexural capacities

The flexural capacities of experimental cases are summarized in Table 3. Except DB2-100 failing by debonding of CFRP sheet, remaining beams were failed in flexural tension in which yielding of strands prior to concrete crushing or CFRP sheet debonding and the sheets were still enacted at the ultimate loads. The detailed results and discussions are following:

(1) Loss of capacities and stiffness due to loss of strand areas

In comparison to CB, the loss of strand areas of 25% (DB1) and 50% (DB2) resulted in the reduction of flexural capacities of 24.9 and 52.5%, respectively. The cracking loads decreased from 62.3 kN in CB to 52 kN in DB1 and 25 kN in DB2. As can be seen from Fig. 3(a), after cracking, the deflections dramatically increased in the damaged beams and there were significant changes in slopes of the curves. The loss concrete portions and ruptured strands caused the member stiffness reduced about 19% (DB1) and 45% (DB2) in pre-cracking region, and 19% (DB1) and 27% (DB2) in post-cracking region.

Table 3 Experimental results

Name	$P_{cr}^{(exp)}$ (kN)	$P_y^{(exp)}$ (kN)	$P_u^{(exp)}$ (kN)	$d_u^{(exp)}$ (mm)	$M_n^{(exp)}$ (kNm)	Reduction of M_n	ε_u' (με)	Pre-cracking stiffness*1 (kN/mm)	Post-cracking stiffness*1 (kN/mm)
CB	62.3	141.36	142.6	26.53	97.60	-	2,733	20.28	4.15
DB1	52.0	105.8	106.5	23.74	73.25	24.9%	NA	16.35	3.37
DB1-100	59.0	122.94	124.7	24.76	85.49	12.4%	2,530	19.48	4.24
DB1-200	60.8	120.18	121.1	21.90	83.07	14.9%	2,670	20.67	4.82
DB1-284	59.6	119.22	120.2	21.46	82.51	15.5%	NA	21.74	5.08
DB1-100U	57.9	123.32	123.8	22.26	84.93	13.0%	2,383	20.22	4.49
DB2	25.0	66.4	66.7	22.52	46.39	52.5%	2,828	11.21	3.05
DB2-100	46.9	82.36	82.4	21.33	56.96	41.6%	2,276	12.55	3.42

P_{cr}, P_y, P_u: cracking, yielding and ultimate load; d_u: deflection corresponding to ultimate load; M_n: flexural capacity; ε_u': strain at top fiber of concrete at ultimate load; NA: not available.
*1: average slope of load-deflection curves of the slope at 60, 70 and 80% of P_{cr} and P_y for pre-cracking and post cracking regions, respectively.

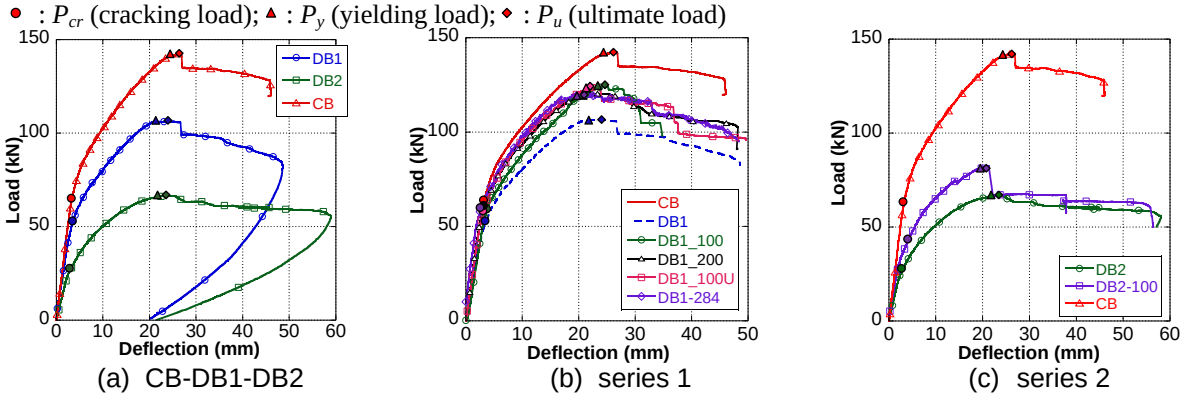

(a) CB-DB1-DB2 (b) series 1 (c) series 2

Fig. 3 Load-deflection curves

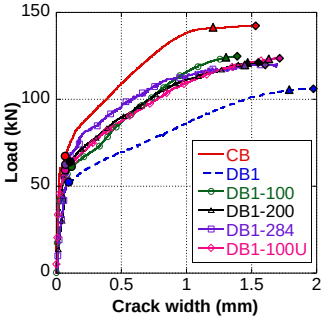

Fig. 4 Load-crack width relationship

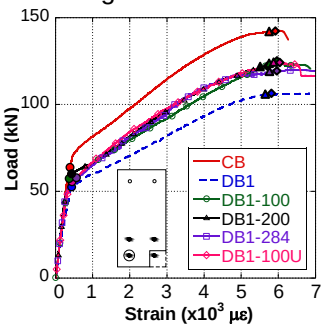

Fig. 5 Load-strain in pre-stressing strands

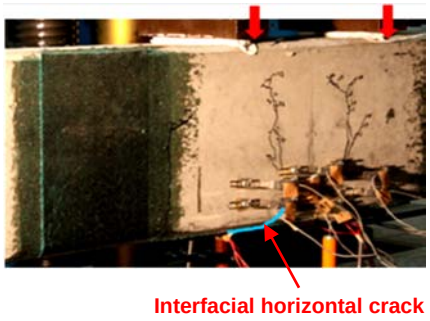

Fig. 6 Interfacial horizontal crack (DB1-100U)

(2) Effects of externally bonded CFRP sheets on the flexural capacities and stiffness

Regarding strengthened beams in series 1, the flexural capacities of beams with CFRP sheets were improved 12.6 to 16.7% in comparison to DB1 but still less than that of CB. There was no noticeable effect of the different lengths of the sheets on the beam capacities. Cracking strengths of beams were recovered up to 95.3% that of CB in average. From load-deflection curves (Fig. 3(b)), the slope of curves changed considerably at cracking loads, then the curves remained approximately linear up to yielding. The slopes in the beams with CFRP sheets illustrate the member stiffness. The post-cracking stiffness increased 38% in comparison to DB1, and enhanced from 2.2% to 22% compared to CB. CFRP sheets represented significant effects on beam stiffness, furthermore, stiffness of beams increased as increasing the lengths of fiber sheets or U-shaped anchorages provided as shown in Table 3. Under four-point loading test, the initial flexural cracks occurred at the constant moment region and progressed upward to the loading points. Since the load continuously increased, other diagonal cracks initiated in the shear span from near loading points to near supports. Since longer CFRP sheet were provided, the cracks, which were located further from the midspan, were restrained. When U anchorages were wrapped, they played the role as similar as stirrups, hence, prevented cracks initiated at the locations where U-shape anchorages were installed. Consequently, the beam stiffness was improved.

Different from series 1, in series 2, the failure of DB2-100 was more brittle, because yielding of prestressing strand followed by debonding of CFRP sheet from the middle of span to the end. This phenomenon indicated the inadequate ratio of steel as

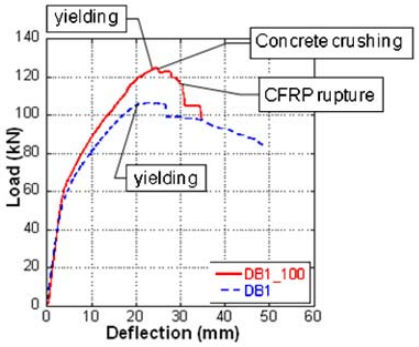

(a) DB1-100

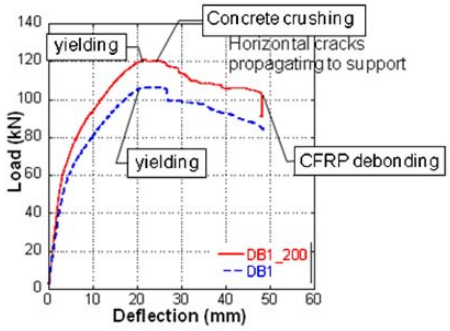

(b) DB1-200

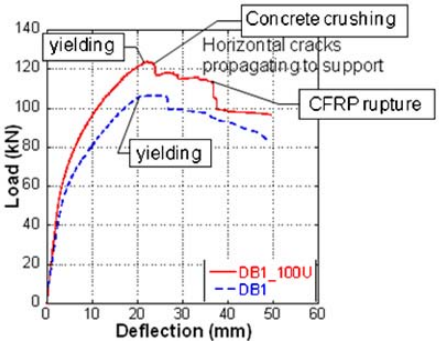

(c) DB1-100U

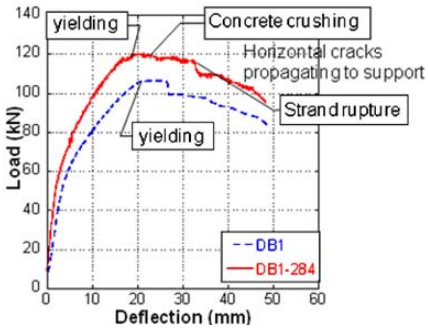

(d) DB1-284

Fig. 7 Post – peak behaviors

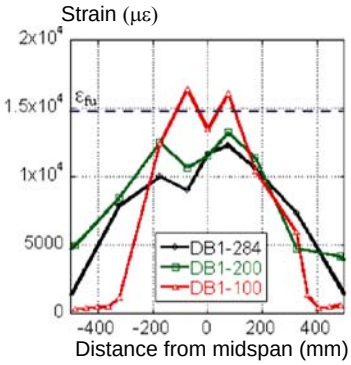

Fig. 8 CFRP strains at ultimate load

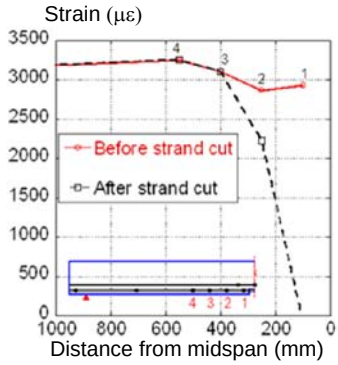

Fig. 9 Strains in ruptured strand (DB1)

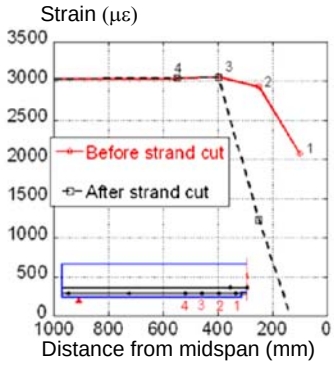

Fig. 10 Strains in ruptured strand (DB2)

well as CFRP sheet and insufficient anchorage length [4]. After delimitation of CFRP sheet, the load capacity of DB2-100 dropped suddenly to the level as similar to that of DB2 where tensile strands yielded. The flexural capacity of DB2-100 increased 22.8% compared to DB2, but it was still far less than that of CB. The load-deflection curves (Fig. 3(c)) depict a large improvement of stiffness not only in post-cracking region but in also pre-cracking region. The stiffness of DB2-100 increased 11.2 to 12.6 kN/mm before cracks occurred, from 3.1 to 3.4 kN/mm after cracking as given in Table 3.

It is likely that after the initial crack occurred, while the concrete in tension no longer supported the load, the bending moment was carried by prestressing strands and CFRP sheets. Because CFRP sheets have maximum lever arm to the neutral axis, they were effective to enhance flexural capacity as well as stiffness of beams.

3.2 Crack widths

By observation, the numbers of cracks were smaller in the beams which strands were cut. The maximum crack openings became larger in damaged specimens as a consequence of loss strand areas. Fig. 4 represents the relationship between applied load and crack openings at near midspan in CB and series 1. At the same load level, cracks opened wider in DB1, and were well restrained with the application of CFRP sheets because in the strengthened beams, bonded fiber sheets carried a part of tensile stress led to the reduction of tensile stresses in strands.

3.3 Tensile strains in prestressing strands

Fig. 5 shows the load-increment of tensile strains at midspan in uncut strands which is circled in legend of series 1. The tensile strains in the prestressing strands in specimens performed similarly before the occurrences of initial flexural cracks. After the first cracks, both prestressing strands and CFRP sheet carried tensile stress, therefore, the tensile stress in prestressing strands exhibited significantly reduction in the strengthened beams. Consequently, the yielding loads were increased around 20% compared to DB1. Effects of the sheet lengths were not recognized clearly in the tensile strains of prestressing strands.

Table 4 Comparisons between experimental results and predicted values

Name	Cracking load			Ultimate load		
	$P_{cr}^{(exp)}$ (kN)	$P_{cr}^{(cal)}$ (kN)	$P_{cr}^{(exp)}/P_{cr}^{(cal)}$	$P_u^{(exp)}$ (kN)	$P_u^{(cal)}$ (kN)	$P_u^{(exp)}/P_u^{(cal)}$
CB	62.28	63.82	0.98	142.60	127.51	1.12
DB1	52.00	46.43	1.12	106.54	96.90	1.10
DB1-100	59.00	49.23	1.20	124.66	118.76	1.05
DB1-200	60.76	46.73	1.30	121.08	121.40	1.00
DB1-284	59.56	46.53	1.28	120.25	120.72	1.00
DB1-100U	57.86	43.19	1.34	123.84	119.56	1.04
DB2	25.00	27.17	0.92	66.74	63.20	1.06
DB2-100	46.90	35.20	1.33	82.40	86.38	0.95

$^{(exp)}$: experimental result; $^{(cal)}$: predicted value

3.4 Failures of composite action

After reaching the ultimate load, the specimens were kept on loading to obtain the post-peak behaviors of composite actions. For DB1-100 (Fig. 7(a)), after yielding of the first strand, the load capacity decreased as concrete crushing. The load capacity, then, had a small rise due to the tensile stress carried by CFRP sheet increased. When tensile stress in CFRP sheet reached its rupture strength, CFRP sheet partially ruptured. The capacity of beams fell off suddenly when CFRP sheet totally ruptured. Thus, fiber sheet had fully utilized its strength in DB1-100.

In case of DB1-100U (Fig. 7(c)), after prestressing strands yielded, flexural cracks in the constant moment region opened widely. A horizontal crack at the interface between concrete and CFRP sheet was initiated from the flexural crack as shown in Fig. 6. Since the applied load still increased, the horizontal cracks propagated to the supports until they were stopped by U-shaped anchorages and the sheet was ruptured. The load decreased sharply at that moment.

Similar to DB1-100U, in DB1-200 (Fig. 7(b)) and DB1-284 (Fig. 7(d)), after strand yielding, the flexural cracks induced the horizontal interfacial cracks. The interfacial cracks propagated to the support as load increased. It led to the debonding of CFRP sheet when it reached the end of the fiber sheet in DB1-200. However, dissimilar behavior was observed in DB1-284, the prestressing strand was ruptured before the horizontal cracks caught the end of CFRP sheet. Hence, there was no occurrence of the delimitation or rupture of CFRP sheet. If interfacial cracks occurred, a sufficient length of CFRP delays peeling process, as a result, post-peak behavior in DB1-284 became more ductile than DB1-200 and DB1-100.

According to this preliminary study, the behavior of composite actions likely related to localized opening of flexural cracks at critical sections. In addition, when the load increased, cracks also propagated around mortar portions resulted in different displacements between concretes and mortar portions. The wide opening of crack widths and different movement of mortar parts caused a vertical displacement in CFRP sheet where the sheet went across the openings or at the edge of mortar portion. This displacement induced a vertical force in CFRP sheet. When this vertical force exceeded the bond strength between concrete and bonded sheet, horizontal crack was created and developed along the interface of concrete and fiber sheet.

3.5 Tensile strains in CFRP sheets

Comparisons in the strains along CFRP sheets at ultimate load have been represented in Fig. 8. In this figure, ε_{fu} illustrates the ultimate strain of CFRP sheet. Maximum strains occurred at location of flexural cracks that was close to the edge of loss concrete portions. Moreover, maximum strains at ultimate load in DB1-200 and DB1-284 were smaller than rupture strain because the appearance of interfacial cracks before the peak loads reduced the effectiveness of composite actions.

3.6 Transfer lengths of cut strands

As it was defined in ACI 318 [2], the transfer length of embedded pre-tensioned strand was required length to transfer the effective prestress to the concrete. In case of strand rupture, the transfer length and transfer of stress were expected to be similar as considering the starting of transfer length at the edge of loss concrete portion. Figs. 9 and 10 illustrate the strains measured in the strands before and after strand cutting in DB1 and DB2. The strains were descended sharply in the length of 350 mm from the edge of concrete. This transfer length (l_{tr}) was smaller than the predicted values (433 mm for DB1 and 379 mm for DB2 corresponding to the designed effective stress of 843 MPa and 737 MPa) based on equations recommended in ACI 318 [2]:

$$l_{tr} = 0.0476 f_{pe} d_b \quad (1)$$

f_{pe}: effective stress in prestressing strand (MPa)
d_b: diameter of prestressing strand (mm)

Although there are many factors affecting the transfer length, for instance, effective stress in the strands, strand cross sections, the surface conditions of strands, concrete strength and concrete cover, the last three factors have not been reflected in the above equation. That explained the difference between predicted and experimental values.

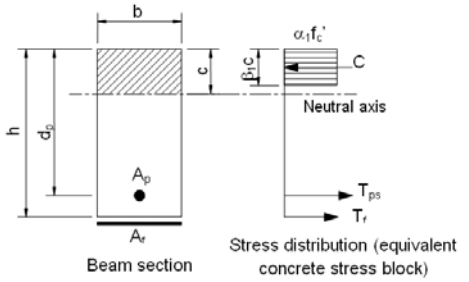

Fig. 11 Stress distribution at ultimate limit state

3.7 Comparisons to ACI codes/guides

The capacities of beams were calculated and compared to the experimental results as shown in Table 4. The capacities of CB, DB1, DB2 were calculated based on ACI 318 [2]:

$$M_n = A_p f_{ps}(d_p - \frac{a}{2}) \quad (2)$$

where

$$a = \frac{A_p f_{ps}}{0.85 f_c' b} \quad (3)$$

A_p: area of prestressing steel
f_{ps}: stress in prestressing steel at beam failure
d_p: effective depth to centroid of prestressing steel
f_c': compressive strength of concrete
b: width of beam

The capacities of the beams with CFRP sheets were predicted based on stress and strain equilibrium method [1]. The equation consists of two components: capacities carried by prestressing strands and fiber sheet:

$$M_n = A_p f_{ps}(d_p - \frac{\beta_1 C}{2}) + A_f f_{fe}(h - \frac{\beta_1 C}{2}) \quad (4)$$

where

f_{fe}: stress in fiber sheet at beam failure, and the other elements are defined in Fig. 11.

However, it is noted that the effects of high concrete strength on behavior of FRP strengthened members and maximum crack width and deflection prediction and control of concrete reinforced with FRP systems have not been developed in the guidelines [1].

While ultimate loads show a good agreement between the experimental results and predictions, cracking loads were underestimated in case CFRP sheets were applied. Thus, the effects of high strength concrete on the composite actions need to be taken into account, particularly, in pre-cracking region. An applicable process for prediction of the capacity of PC beams with externally bonded CFRP sheets need to be further investigated.

4. CONCLUSIONS

(1) The externally bonded CFRP sheets showed effective performances in improvement of the flexural capacities and recovery of the stiffness of the PC beams with strands ruptured. The crack widths were controlled and tensile strains in prestressing strands became smaller at the same loads. However, the sufficient ratio of CFRP sheets to restore the original capacity of the damaged beams needs to be further studied.

(2) Increase of the length of CFRP sheets was not effective in the flexural capacities but enhanced beam stiffness because of restraining crack opening effects of CFRP sheets. Post-peak behaviors became less brittle with the longer sheets in case interfacial cracks occurred.

(3) Providing U-shaped anchorages at both ends of flexural sheet efficiently prevented CFRP sheet from debonding, and changing the failure mode from debonding to rupture of CFRP sheet. The beam stiffness was also improved in comparison to the beam bonded the same length CFRP sheet but without the end anchorages.

(4) The transfer lengths in ruptured strand were investigated. From the experimental results, the actual transfer lengths were smaller than predicted values based on ACI [2] recommendations because concrete strength and concrete cover have not been considered in the predicted equations.

(5) The calculated flexural capacities based on ACI guidelines [1, 2] showed good agreements for ultimate loads. Nevertheless, the cracking loads were underestimated. The effects of CFRP sheets on high strength concrete need to be considered in prediction PC beam capacity.

REFERENCES

[1] ACI, “Guide for the Design and Construction of Externally Bonded FRP Systems for Strengthening Concrete Structures”, ACI 440-2R, ACI Committee 440, 2008

[2] ACI, “Building Code Requirements for Structural Concrete and Commentary”, ACI 318, ACI Committee 318, 2008, pp. 119-128, pp. 281-308

[3] Thomsen, H. et al., “Failure mode analysis of reinforced concrete beams strengthened in flexural with externally bonded fiber-reinforced polymers”, Journal of Composites for Construction, ASCE, Apr. 2004, pp.123-131

[4] Harries, K. A., “Repair method for prestressed girder bridges”, Technical report, Pennsylvania Department of Transportation, Jun. 2009

[5] Wu, Z. et al., “State-of-the-Art of advanced FRP applications in civil infrastructure in Japan”, Composites and Polycon 2007, American Composites Manufactures Association, Oct. 17-19, 2007

[6] Toutanji, H. et al., “Flexural behavior of reinforced concrete beams externally strengthened with CFRP sheets bonded with an organic matrix”, Engineering Structures 28, 2006, pp. 557-566

[7] Anania, L. et al., “Increasing the flexural performance of RC beams strengthened with CFRP materials”, Construction and Building Materials 19, 2005, pp. 55-61